Corrosion Thickness Characterization in Steels by Means of Active Thermography

Original
Corrosion Thickness Characterization in Steels by Means of Active Thermography / Cura', F.M., Sesana, R., Dugand, M.M.. - ELETTRONICO. - 254:(2023), pp. 570-577. (10th European Workshop on Structural Health Monitoring, EWSHM 2022 italia, palermo 2022) [10.1007/978-3-031-07258-1_58].

Publisher:
Springer Science and Business Media Deutschland GmbH

Published
DOI:10.1007/978-3-031-07258-1_58

Corrosion Thickness Characterization in Steels by Means of Active Thermography

Francesca Curà[1], Raffaella Sesana[1](✉), and Marie Marguerite Dugand[2]

[1] Dimeas Politecnico di Torino, Corso Duca degli Abruzzi 24, 10129 Turin, Italy
`raffaella.sesana@polito.it`

[2] CRF - Materials Engineering Methods and Tools, E/E and Multifunctional Materials - Opto-Electronic and Glazing, C.so Settembrini 40, 10235 Turin, Italy

Abstract. The present work concerns the study of distributed defects on metal surfaces. A typical situation is represented by corrosion due to environmental effect, for example in pipings. In this case, the detection of both presence and corrosion amount inside piping is difficult and often requires the use of non-destructive techniques. Aim of this work is the feasibility analysis of active thermography for non-destructive detection and quantification of corrosion in steel sheets. In particular, the present work aims at developing a data processing technique for thermal results obtained on steel sound and coroder sheets by means of a laser thermal investigation. Both pulsed and lock in active thermography techniques are explored, in transmission configuration. The influence of excitation parameters on damage detection and quantification performance was also investigated. To this aim different samples of specimens were obtained with increasing corrosion damage, by means of keeping the specimens in a saline cell for increasing time intervals. For all the investigations, the reference signal consisted in the sound sheet thermal response. Data processing allowed to relate frequency and time parameters of the thermal response to the corrosion level. The entity of corrosion was also compared to the thickness specimen variation obtained by means of a metallographic optical microscope.

Keywords: NDT · Active thermography · Corrosion

1 Introduction

Corrosion phenomena may affect almost all metals and they are critical for structural integrity of components during their life. Primary goal for engineers is the detection of corrosion, in particular the hidden corrosion presence and the corresponding metal loss.

Corrosion detection and monitoring is a challenge for researchers and industries and a lot of experimental techniques were developed over the years to achieve this purpose. Non Destructive Techniques (NDT) as Infrared Thermography (IRT) were widely used to generally detect defects, concentrated and distributed, and to characterize the entity of damage in both qualitative and quantitative point of view.

P. Rizzo and A. Milazzo (Eds.): EWSHM 2022, LNCE 254, pp. 570–577, 2023.
https://doi.org/10.1007/978-3-031-07258-1_58

For as concerns specifically corrosion detection, a thorough overview on the applications of Infrared Thermography for the detection and characterization of general metal loss in metallic materials is reported in [1].

Infrared Thermography techniques may be classified into two major categories: active thermography, that requires an external excitation source, and passive thermography, that doesn't require an external source as the object presents naturally a thermal contrast with respect to the rest of the scene. External sources for active thermography may be optical (photographic flashes and Halogen lamps, laser) or inductive (electro-magnetic coils) [1, 2].

From the excitation point of view, optical excitation mainly refers to two classical active thermographic techniques: lock-in thermography and pulsed thermography [3, 4], each one characterised by its peculiarities [5].

In general, optical excitation thermographic techniques (above all pulsed and lock-in thermography), were used to detect defects of various shapes, origins and positions, with particular attention not only to external sources and excitations typologies, but also to the corresponding data processing techniques.

As some examples, ability of thermography to detect defects in composite materials [6] or delamination in CFRP [7] was demonstrated. Lock-in was widely used in electronic device testing, to enable the localization of very weak local heat sources below the surface [8].

For as concerns the detection of corrosion, object of this paper, it has to be considered that, in case of inspecting structures for hidden corrosion, there is normally no access to inspect from the corroded side, the majority of research associated with metal loss defect detection are characterized with both camera and excitation source located at the front surface of the specimen [1]. Such configuration is known as reflection configuration, compared to the transmission one in which the heat source is located at the opposite side of the camera behind the specimen front surface.

A novel method was recently patented [9] to detect corrosion on a surface not exposed to view of a metal piece, by utilizing an active thermographic approach, in particular directing the radial thermal energy against the piece by pulsed laser beam illumination.

Aim of the present work is to investigate the corrosion entity and the corresponding metal loss in metal sheets by active thermography in transmission configuration [9].

In particular, the present work aims at developing a data processing technique for thermal results obtained on steel sound and corroder sheets by means of a laser thermal investigation. Both pulsed and lock in active thermography techniques are explored, in transmission configuration. The influence of excitation parameters on damage detection and quantification performance was also investigated.

To this aim different samples of specimens were obtained with increasing corrosion damage, by means of keeping the specimens in a saline cell for increasing time intervals.

The entity of corrosion was also compared to the thickness specimen variation obtained by means of a metallographic optical microscope.

2 Materials and Methods

Tests were run on three specimens obtained from a laminated Al steel. Two specimens were positioned in a saline cell and on each specimen one surface was protected while the other one underwent a saline fog (5% NaCl) for 2 weeks and 4 weeks respectively, while the third specimen was left uncorroded. In Fig. 1 two of the specimens are presented.

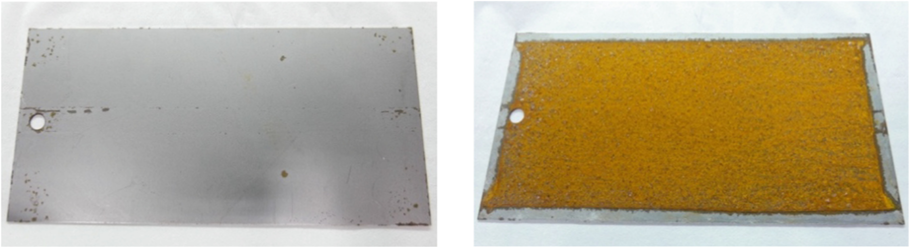

(a) (b)

Fig. 1. Specimens uncorroded (a) and corroded (b)

An infrared Flir X6540sc cooled sensor IR camera was used, in an integrated Laser DES Active Thermography system. A Laser IPG YLP-V2 30 W power was used as excitation source.

Lock in and Pulsed square wave thermal loading tests were run on specimens. Excitation parameters were varied as reported respectively in Tables 1 and 2.

Table 1. Excitation parameters for Lock in tests

Test name	Corrosion time [week]	Excitation time [ms]	Excitation power %	Acquisition frame rate [Hz]
A	0, 2, 4	200	100	540
B	0, 2, 4	200	50	540
C	0, 2, 4	200	25	540
D	0, 2, 4	2000	25	540
E	0, 2, 4	1000	25	108

Table 2. Excitation parameters for Pulsed tests

Test name	Corrosion time [week]	Excitation time [ms]	Excitation power %	Acquisition frame rate [Hz]
F	0, 2, 4	1000	100	400
G	0, 2, 4	1000	50	400
H	0, 2, 4	1000	25	400
L	0, 2, 4	200	100	400
M	0, 2, 4	500	100	400

For each specimen, three points were investigated and three repetitions per point were run. Thermal contours evolution with time were acquired in each point and for each repetition.

Phase and amplitude average of thermal signals were computed and plotted for each testing configuration. These plots were compared for different corrosion conditions and different acquisition configurations. An example of a Phase signal computed in the instant when the maximum temperature is obtained, is reported in Fig. 2. For Lock in tests, in the same figure, two parameters selected for a deeper analysis are shown: peak and valley distance in the plot, in this case for the first harmonic.

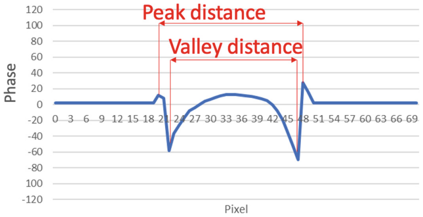

Fig. 2. Example of phase plot in Lock in tests

Figure 3 shows an example of heating and cooling plot for Pulsed Tests (laser target point). For Pulsed tests the slopes of heating and cooling time curve, in space, were calculated. These parameters were compared for different corrosion conditions and different acquisition configurations.

Furthermore, a micrographic analysis was run to quantify the variation in thickness of the specimen with corrosion increment and to estimate the corroded surface density evolution.

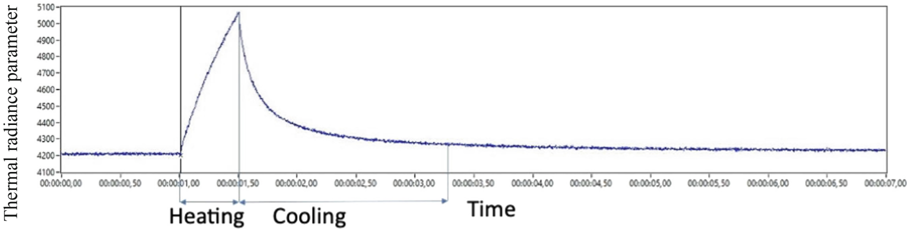

Fig. 3. Example of heating and cooling plot for Pulsed Tests (laser target point)

3 Results and Discussion

Table 3 resumes the thickness specimen variation obtained by means of a metallographic optical microscope in order to characterize the entity of corrosion.

Table 3. Level of corrosion and material thickness

Level of corrosion	Material thickness [mm]
Non corroded	0,76 ÷ 0,90
2 weeks	0,72 ÷ 0,95
4 weeks	0,60 ÷ 0,76

Results obtained for some testing configurations are resumed in Figs. 4, 5, 6, 7, 8 and 9. More in detail, Figs. 4, 5 and 6 refer to Lock in tests, while Figs. 7, 8 and 9 refer to pulsed ones.

Figure 4 shows the first harmonic thermal amplitude for test A (a) and for test E (b) (see Table 1 for test parameters characterization). For both A and E configurations, the blue curve corresponds to the non-corroded condition, orange and grey curves refer to the corroded conditions obtained respectively during 2 and 4 weeks in a saline cell.

Corresponding maximum thermal amplitude values for the first harmonic are shown in Fig. 5 as a function of the laser power (a) and of the impulse duration (b). Blue, orange and grey data correspond to the conditions already mentioned for Fig. 4 (non corroded, 2 and 4 weeks corrosion respectively).

Figure 6 resumes the first harmonic phase distances for tests A (a) and E (b). This information, in terms of number of pixel between peaks (blue curve) and valleys (orange curve) of the phase plot respectively, is reported as a function of the corrosion time (weeks).

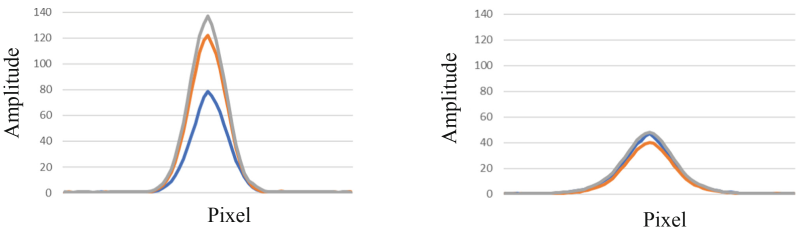

(a) (b)

Fig. 4. Lock in test: first harmonic amplitude for test A (a) and test E (b) (blue non corroded, orange 2 weeks corrosion, grey 4 weeks corrosion).

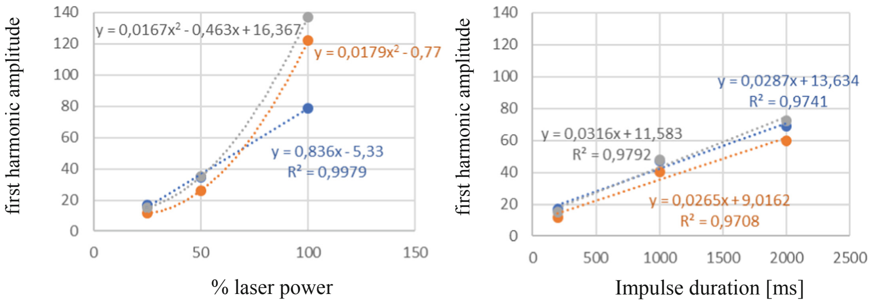

(a) (b)

Fig. 5. Lock in tests: first harmonic amplitude vs laser power (a) and impulse duration (b) (blue non corroded, orange 2 weeks corrosion, grey 4 weeks corrosion).

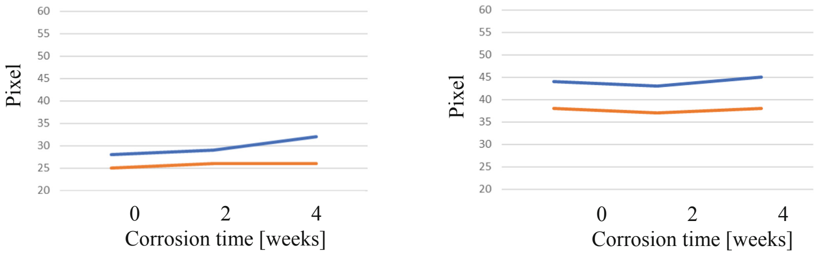

(a) (b)

Fig. 6. Lock in tests: first harmonic phase distance vs corrosion week: test A (a) and Test E (b) (blue between peaks, orange between valleys).

Different peculiarities of thermal signals, as already emphasized in Fig. 3, are needed in presenting the results of Pulsed tests.

Figure 7 shows the curve slopes related respectively to heating (a) and cooling (b) for test A (blue non corroded, orange 2 weeks corrosion, grey 4 weeks corrosion). The maximum heating curve slope as a function of the excitation power (a) and of the impulse duration (b) is shown in Fig. 8 (color curves correspond to those of Fig. 7, blue non corroded, orange 2 weeks corrosion, grey 4 weeks corrosion).

Finally, the maximum cooling curve slope as a function of the excitation power (a) and of the impulse duration (b) is shown in Fig. 9 (color curves corresponding to Figs. 7 and 8).

From the analysis of Figs. 4, 5 and 6 related to Lock in results, it can be observed that testing conditions have to be carefully tuned in order to emphasize the corrosion entity.

From the signal amplitude point of view, the first harmonic was correctly chosen as representative of the damaging condition (see Fig. 4), but its level better points out the corrosion degree if a high power of the laser excitation was chosen (test A). Figure 5 emphasises this aspect, showing that a higher laser power increases the thermal signal amplitude for all corrosion conditions. The amplitude level is also influenced by the impulse duration (Fig. 5), but it is not so sensitive to the corrosion entity.

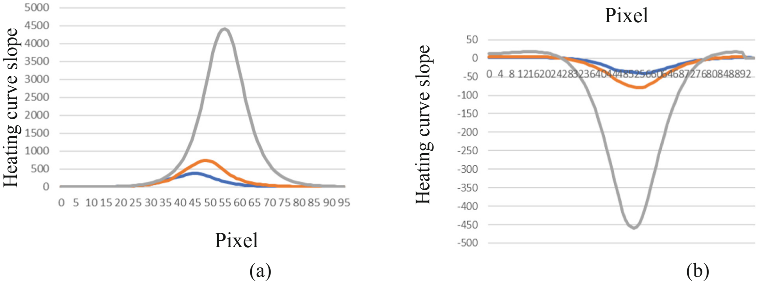

Fig. 7. Pulsed test: Heating curve slope (a) and cooling curve slope (b) for test F (blue non corroded, orange 2 weeks corrosion, grey 4 weeks corrosion)

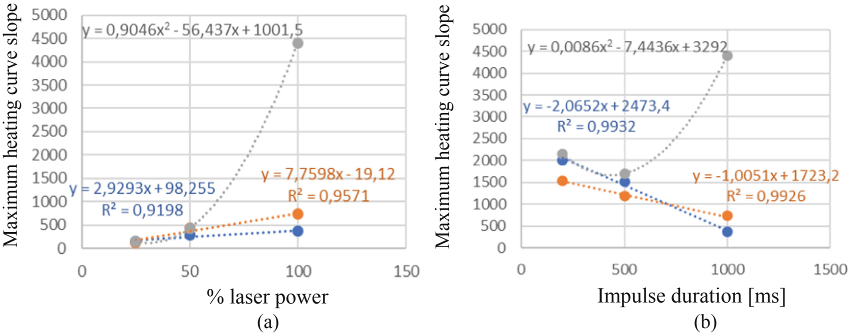

Fig. 8. Pulsed test: maximum heating curve slope vs excitation power (a) and impulse duration (b) (blue non corroded, orange 2 weeks corrosion, grey 4 weeks corrosion)

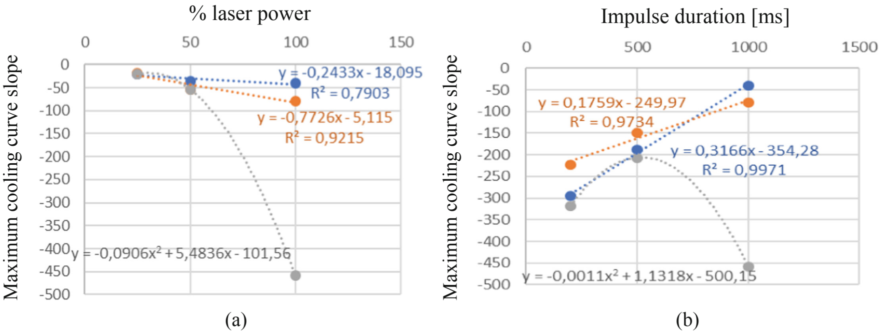

Fig. 9. Pulsed test: maximum cooling curve slope vs excitation power (a) and impulse duration (b) (blue non corroded, orange 2 weeks corrosion, grey 4 weeks corrosion)

From the signal phase point of view (first harmonic), as indicated in Fig. 6, only the distance between peaks can be considered as sensitive to the corrosion entity.

Results of Figs. 6, 7 and 8 related to pulsed tests follow the same logic, being strongly sensitive to the testing conditions, above all the laser source power. The reference parameters are the slopes of heating and cooling curves, both showing the effect of corrosion if a high-power excitation was chosen (Fig. 7, Table 2, test F).

Similar comments arise from the analysis of Figs. 8 and 9, reporting respectively the maximum heating and cooling curves slope as a function of testing parameters, laser power and time duration. These parameters strongly influence the method capability to detect the corrosion, showing that the effect of corrosion is better identified by a variation of the exciting source power.

4 Conclusions

The present paper aimed at demonstrating the feasibility analysis of active thermography for non-destructive detection and quantification of corrosion in steel sheets.

On the basis of the obtained results, some conclusions can be drawn in the following.

Active thermography technique in reflection configuration can be satisfactorily utilized to detect and quantify surface distributed defects as corrosion damage, provided that the best tuning for testing parameters can be reached.

This need is strictly related to the measurements difficulties and uncertainties related to the non-uniform corrosion distribution on the specimens, causing a signal scattering related to density and reflecting surfaces variation.

Future developments will require the optimization of active thermography testing parameters, in order to guarantee the robustness of this technique, even if the actual difficulty in this approach is represented by the uncertainty in thickness punctual values of corroded specimens that makes difficult a quantitative comparison to thermal parameters variation.

References

1. Doshvarpassanda, S., Wub, C., Wang, X.: An overview of corrosion defect characterization using active infrared thermography. Infrared Phys. Technol. **96**, 366–389 (2019)
2. Osvald-Tranta, B.: Lock-in inductive thermography for surface crack detection in different metals. Quant. InfraRed Thermography J. **16**(3–4), 276–300 (2019)
3. Ibarra-Castanedo, C., Maldague, X.: Pulsed phase thermography reviewed. QIRT J. **1**(1), 47–70 (2004)
4. Rajic, N., Antolis, C.: An investigation of noise performance in optical lock-in thermography. Infrared Phys. Technol. **87**, 1–10 (2017)
5. Rajic, N., Antolis, C.: Optical lock-in thermography for structural health monitoring – a study into infrared detector performance. Proc. Eng. **188**, 471–478 (2017)
6. Palumbo, D., Cavallo, P., Galietti, U.: An investigation of the stepped thermography technique for defects evaluation in GFRP materials. NDT & E Int. **102**, 254–263 (2019)
7. Liu, B., Zhang, H., Fernandes, H., Maldague, X.: Experimental evaluation of pulsed thermography, lock-in thermography and vibrothermography on Foreign Object Defect (FOD) in CFRP. Sensors **16**, 743 (2016)
8. Breitenstein, O., Sturm, S.: Lock-in thermography for analyzing solar cells and failure analysis in other electronic components. Quant. InfraRed Thermography J. **16**, 203–217 (2019)
9. Dugand, M.M., et al.: Method for detecting corrosion on a surface not exposed, by means of thermographic analysis. Patent No.: US 10, 145,800 B1 (2018)